JOURNAL OF CATALYSIS **174,** 72–87 (1998)
ARTICLE NO. CA971960

Hardness and Salt Effects on Catalytic Hydrogenation of Aqueous Nitrate Solutions

Albin Pintar,*,[1] Marko Šetinc,* and Janez Levec*,†

*Laboratory for Catalysis and Chemical Reaction Engineering, National Institute of Chemistry, Hajdrihova 19, P.O. Box 3430, SI-1001 Ljubljana, Slovenia; and †Department of Chemical Engineering, University of Ljubljana, Aškerčeva 5, P.O. Box 537, SI-1001 Ljubljana, Slovenia

Received July 24, 1997; revised October 9, 1997; accepted October 9, 1997

Liquid-phase hydrogenation using a solid Pd–Cu bimetallic catalyst provides a potential technique for the removal of nitrates from waters. In this study, hardness and salt effects on both the nitrate disappearance rate and the reaction selectivity were quantitatively evaluated. Reduction experiments were performed for a wide range of nitrate conversions in an isothermal semibatch slurry reactor. It was discovered in a series of runs using various nitrate salts as a source of nitrate ions that the apparent surface reaction rate constant increases in the order $K^+ < Na^+ < Ca^{2+} < Mg^{2+} < Al^{3+}$ and changes proportionally with the ionization potential of a cation present in the aqueous solution. Permanent hardness of drinking water exhibits no inhibitive impact either on the extent of nitrate removal or on reaction selectivity. On the other hand, the nitrate disappearance rate as well as nitrogen production yield decrease appreciably in the presence of hydrogencarbonates, which is attributed to identical structures of nitrate and hydrogencarbonate ions resulting in competitive adsorption of these species to Pd–Cu active sites. A detailed analysis of experimental data confirmed that efficiency of the Pd–Cu bimetallic catalyst in catalytic nitrate reduction is influenced by the migration of produced hydroxide ions from the Helmholtz layer. © 1998 Academic Press

INTRODUCTION

Groundwater pollution by nitrates, which are perhaps the most ubiquitous of all groundwater contaminants, is a widespread problem in many locations in the world. Man-made or man-induced sources of nitrogen introduction into the subsurface environment include agricultural fertilizers, septic tank systems, and animal waste disposal. A number of hydrogeological factors and agricultural practices like precipitation/runoff, irrigation, soil type, and depth and geological features such as karst areas, denitrification, fertilizing intensity, crop types, and land usage influence the concentration of nitrates in groundwater at specific locations. Canter (1) and Sell *et al.* (2) provide statistical data which represent the extent of drinking water contamination by nitrates in United States and European countries. It is reported by the first author that for some locations nitrate concentration in water has been found to be at risky levels up to 200 mg/L. Since this value is excessively above the admissible concentration (i.e., 50 mg/L) set by the European Drinking Water Directive, the nitrate content in such streams should be necessarily reduced in order to avoid health risk. The toxicity of nitrates to humans is due to the body's reduction of nitrate to nitrite. The role of the latter as a precursor to clinical cyanosis (blue baby syndrome) and carcinogenic nitrosamines as well as to other *N*-nitroso compounds is firmly established (1).

Conventional physicochemical methods (e.g., ion exchange, reverse osmosis, and electrodialysis) allow effective removal of nitrate ions from contaminated groundwater, however, by concentrating them in a secondary waste stream, which has called for new, compact, and environmental friendly systems. The most promising techniques for nitrate removal, without any occurrence of wastewater, are biological digestion (3) and catalytic denitrification by using noble metal catalysts (4–6). Biological denitrification processes (either heterotrophic or autotrophic) are known to have great potential for the treatment of municipal and industrial wastewater streams. The main reasons for the slow transfer of technology to drinking water purification are concerns over possible bacterial contamination of treated water, the presence of residual organics in treated water, and the possible increase in chlorine demand of purified water. The reduction of aqueous nitrate solutions by using hydrogen over a solid catalyst offers an alternative and economically advantageous process to biological treatment as a means of purifying drinking water streams. In this process, which can be represented by the overall reaction

$$2NO_3^- + 5H_2 \xrightarrow{Pd-Cu/\gamma\text{-}Al_2O_3} N_2 + 2OH^- + 4H_2O, \qquad [1]$$

nitrates are selectively converted via intermediates to nitrogen in a two- or three-phase reactor operating under mild reaction conditions (e.g., T, 278–298 K, p_{H_2} up to 7 bar (2)).

[1] To whom correspondence should be addressed. Fax: +386 61 1259244. E-mail: albin.pintar@ki.si.

0021-9517/98 $25.00
Copyright © 1998 by Academic Press
All rights of reproduction in any form reserved.

To maintain electroneutrality of the aqueous phase, nitrates are replaced by hydroxide ions. Supported Pd–Cu bimetallic catalysts exhibit the highest activity for nitrate reduction and chemical resistance, but still inadequate selectivity toward nitrogen production. The main drawback of these solids is formation of the side product, ammonia, which is undesirable in drinking water. Since catalytic liquid-phase hydrogenation of aqueous nitrate solutions is in a stage of development, it is obvious that more kinetic and mechanistic studies in aqueous solutions are needed in order to develop an effective catalytic process for purifying drinking water streams and industrial effluents.

Relatively few investigations have been published on the reduction of nitrates in aqueous solutions. It is reported by Hörold *et al.* (6, 7) that Pd hydrogenation catalysts doped by Cu represent the most active and selective bimetallic solids for the transformation of nitrates to nitrogen. The potential of Pd–Cu catalysts for liquid-phase nitrate hydrogenation was studied by these authors at $T = 283$ K in a slurry reactor sparged by pure hydrogen. For the initial nitrate concentration set to 100 mg/L, the reaction selectivity was found to be at a level of 82 mol%. This value could be further increased by carrying out the reaction at lower hydrogen concentrations over a mixture of supported Pd–Cu and Pd catalysts (6). In this way, it was possible to reduce 100 mg/L of nitrate without exceeding the European Community permitted level of ammonia in drinking water (i.e., 0.5 mg/L). Hörold *et al.* (7) have also proposed that the catalytic nitrate reduction, similarly to the autotrophic–chemolitotrophic denitrification with microorganisms, undergoes a stepwise transformation of the parent ion via intermediates (such as NO and N_2O) to nitrogen and ammonia. In agreement with these observations, Wärnå *et al.* (8), who performed measurements in a metallic monolith reactor, suggested that in the process of catalytic nitrate reduction the key intermediate on a noble metal surface might be NO. Pintar and Kajiuchi (9) studied the same reaction in the presence of various Pd–Cu bimetallic catalysts which were prepared according to different impregnation sequences of γ-Al_2O_3 support. The results showed that the nitrate to nitrite reduction step undergoes a structure-insensitive reaction. Furthermore, it was indicated that the overall reaction selectivity is adversely affected by the amount of nitrite ions accumulated in the liquid phase. It has been recently discovered that the selectivity of the reaction under consideration strongly depends on the spatial distribution of Pd and Cu metallic phases, which is confirmed by AES profiling (10). Among all Pd–Cu bimetallic solids tested in a semibatch slurry reactor, the highest reaction selectivity (i.e., over 90 mol% for the initial nitrate concentration equal to 200 mg/L) has been obtained for the catalyst sample in which the metallic copper phase was coated by a Pd layer. Similar behavior with respect to minimum nitrite accumulation was reported also for Pd–Cu bimetallic catalysts synthesized by using a sol-gel preparation procedure (11). However, the obtained reaction selectivities were found to be as low as 60 to 75 mol%, which was probably caused by inappropriate textural properties of these materials. It has been reported very recently by Prüsse *et al.* (12) that alumina-supported Pd–Zn, Pd–Sn, and Pd–In bimetallics prepared by different methods promote liquid-phase nitrate reduction enabling a moderate level of nitrogen formation. When Pd–Sn/Al_2O_3 solids are synthesized by a deposition–precipitation procedure, high reaction selectivities are obtained, however, at the expense of the length of catalyst life period. Prüsse *et al.* (13) report also that formic acid, which is *in situ* transformed to H_2 and CO_2, can be efficiently employed as a reductant in the process of catalytic nitrate hydrogenation.

Quantitative rate data concerning the catalytic liquid-phase nitrate reduction are meager. Tacke and Vorlop (14) determined the kinetics of nitrate hydrogenation over a Pd–Cu bimetallic catalyst containing 5 wt% of Pd and 1.25 wt% of Cu. The measurements were performed in a slurry reactor at $T = 283$ K. The initial rate kinetic data they analyzed resulted in the rate expression of power-law type. They found the reaction rate to be of 0.7 order with respect to nitrate and independent of hydrogen partial pressure provided that this pressure is greater than about 1.0 bar. It is further reported that the observed rate per unit weight of catalyst is not affected by the catalyst concentration. Recently, a detailed kinetic model of the catalytic nitrate reduction was derived by Pintar *et al.* (15). The rate of nitrate disappearance has been well described by a rate equation of the Langmuir–Hinshelwood type, which accounts for both noncompetitive and equilibrium nitrate and dissociative hydrogen adsorption steps as well as an irreversible bimolecular surface process that controls the overall reaction rate. The observed kinetics in the slurry reactor are not influenced by the presence of nitrites as intermediates in the reduction route toward nitrogen formation. Furthermore, the change of pH value of aqueous solution during the reaction course has a minor influence on the nitrate disappearance rate. The authors have also reported that the liquid-phase reduction of aqueous nitrate solutions over supported Pd–Cu bimetallics occurs by a heterolytic electron transfer between adsorbed reactant species on different types of active sites.

In the investigations discussed above, KNO_3 and distilled (or deionized) water have been employed so far as a source of nitrate ions and a reaction medium, respectively. Our preliminary experiments have shown that the nitrate disappearance rate is substantially influenced by the composition of the liquid phase. The objective of this work is to provide reaction rate data obtained in the presence of various cations in the aqueous solution as well as to investigate the potential effects of hardness and ionic strength of the liquid phase on the reaction progress. The measurements were

conducted in an isothermal semibatch slurry reactor in the presence of a Pd–Cu bimetallic catalyst. A few reduction runs were carried out by using tap water instead of distilled water in order to evaluate the potential of the catalytic denitrification technique for drinking water purification. The values of kinetic parameters, included in a rate equation of the Langmuir–Hinshelwood type, typical of heterogeneous catalytic systems, were derived by means of an integral kinetic analysis. The results obtained are discussed in terms of the processes that take place at the catalyst–electrolyte interface.

EXPERIMENTAL

Catalyst Preparation

The liquid-phase reduction of aqueous nitrate solutions by hydrogen was studied using a Pd–Cu bimetallic catalyst. A powdered γ-Al_2O_3 from Nikki-Universal (NST-3H type; surface area (BET method), 154 m^2/g; average particle diameter, 25 μm; pore diameter, 10–25 nm) was employed as a carrier of active components. Copper and palladium nitrates were selected as precursors for the sample preparation; both salts were deposited from aqueous solutions. The following sequences of wet impregnation were employed during the catalyst preparation procedure: (i) impregnation by copper nitrate; (ii) drying in an oven at $T = 423$ K and calcination in air for 1 h at $T = 773$ K; (iii) deposition of palladium nitrate followed by drying at $T = 423$ K. Finally, the resulting solid was calcined for 3 h in air at $T = 773$ K and then reduced in hydrogen atmosphere for 1 h at the same temperature. The concentrations of metallic Pd and Cu phases were equal to 4.7 and 1.4 wt%, respectively. The surface area (BET method) of the Pd–Cu bimetallic catalyst was 142 m^2/g, while the isoelectric point, obtained from electrophoretic mobility and streaming potential data, was equal to 8.8. The XRD pattern of the Pd–Cu catalyst evidenced only peaks due to alumina (γ-form). No peaks assigned to palladium or copper containing phases were detected, thus suggesting the presence of highly dispersed metallic phases which was also confirmed by EDAX examination. A comparison of X-ray diffractograms of the alumina support and Pd–Cu bimetallic catalyst shows that the catalyst preparation procedure mainly influences the peak position at 2Θ close to 40°, which can be attributed to the preferred diffusion of Pd and Cu atoms into the γ-Al_2O_3 lattice (11, 16).

Apparatus and Experimental Procedure

Measurements were carried out in a 2.0-L reactor made of Pyrex glass and equipped with a stirrer and temperature control unit. Since the liquid-phase nitrate reduction can also be promoted by physical mixtures consisting of supported hydrogenation catalysts and metallic particles (9, 10), the reactor was free of metal parts in order to eliminate their effects on measured nitrate conversions. The temperature of the reaction mixture was successfully controlled within ± 0.1 K of the set value by employing a PID control. No temperature rise, due to the heat of reaction, was observed in any of the runs because the reactor was operated with low nitrate concentrations (up to 100 mg/L). No pressure control was required since the total operating pressure was equal to atmospheric pressure. The hydrogen and nitrogen flows, introduced into the vessel below the impeller, were controlled by electronic mass flow controllers. Three phases were present in the reactor, so the entire system is treated as a slurry reactor.

TABLE 1

Range of Reaction and Operating Conditions of the Catalytic Liquid-Phase Nitrate Hydrogenation Carried Out in the Slurry Reactor

Reaction temperature, K	298
Hydrogen partial pressure, bar	0.1, 0.4
Total operating pressure, bar	1.0
Catalyst concentration, mg/L	150
Average catalyst particle diameter, μm	25
Initial nitrate concentration, mg/L	100.0
Ionic strength, mmol/L	1.6–25.0
Stirrer speed, rpm	550
Gas flow rate, mL_n/min	500
Reaction volume, L	1.5

The range of experimental conditions used in this work is listed in Table 1. It has been already demonstrated previously that given these reaction conditions both external as well as internal mass-transfer resistances are negligible (15). In a typical run, a given amount of fresh (and previously reduced) catalyst was charged into the reactor containing 1.4 L of distilled water. The content of the reactor was purged with nitrogen and then continuously sparged with a mixture of hydrogen and nitrogen at a metered rate. In some hydrogenation runs, carbon dioxide was employed as hydrogen diluting agent. When the temperature of the reactor system was constant and equal to the set value, a concentrated solution (100 mL) of nitrates was introduced into the slurry. The following reagent-grade compounds were employed as a source of nitrate ions: KNO_3, $NaNO_3$, $Ca(NO_3)_2$, $Mg(NO_3)_2$, and $Al(NO_3)_3$. To monitor the progress of the reaction, representative samples were withdrawn periodically and the catalyst was immediately separated from the aqueous phase by centrifugation. The aqueous phase was then analyzed for residual contents of nitrates as well as instantaneous concentrations of nitrite and ammonium ions. When effects of temporary and permanent hardness on the reaction course were investigated, respective chlorides, sulphate, hydrogencarbonates, or carbonates were added into the aqueous solution prior to starting a reduction run. In these cases, KNO_3 was employed as a reactant. Furthermore, some experiments were conducted

TABLE 2

Composition of Tap Water Used as a Reaction Medium in the Process of Catalytic Liquid-Phase Nitrate Hydrogenation

Component	Concentration, mg/L
Potassium (K^+)	1.4
Sodium (Na^+)	3.5
Ammonium (NH_4^+)	0.15
Calcium (Ca^{2+})	70.8
Magnesium (Mg^{2+})	17.1
Chloride (Cl^-)	5.6
Hydrogencarbonate (HCO_3^-)	267
Nitrate (NO_3^-)	14.6
Nitrite (NO_2^-)	<0.02
Sulfate (SO_4^{2-})	19
Total organic carbon (TOC)	0.6

in which tap water was used as a reaction medium instead of distilled water; the composition of the former is given in Table 2.

Analysis

The concentrations of nitrate ions in the aqueous-phase samples were determined by employing a UV/VIS spectrophotometer (Perkin-Elmer, Model Lambda 40P) combined with the X–Y autosampler and flow-injection analyzer (Perkin-Elmer, Model FIAS 300). A flow cell with a volume of 18 μL and optical pathlength of 10 mm was installed in the sample compartment of UV/VIS spectrophotometer, thus enabling instantaneous response. The nitrate ions analysis was carried out in the UV range at $\lambda =$ 220 nm. Distilled water was used as a mobile phase, and the flow rate of the latter was set to 240 mL/h in order to ensure linear system response in the concentration range 0–250 mg/L of nitrates. Reagents containing diluted perchloric (2.5 wt%) and amidosulfuric (1.0 wt%) acids were employed as a means to eliminate any effect of the present nitrite ions on the measured absorbances (17). The flow of the mobile phase and reagents through the tubing and loops was arranged in such a way that a sample was injected accordingly to the branched flow injection analysis (FIA) technique. For the described analytical method, the relative analysis error was found to be below 0.5%. To evaluate concentrations of nitrite and ammonium ions, the "naphthylamine" and "gas-diffusion" analytical procedures were applied using the same apparatus. In some liquid-phase nitrate reduction experiments, a temporal course of chloride, sulfate and hydrogencarbonate ions was also followed. While the concentrations of chlorides and sulfates were evaluated by means of UV/VIS–FIA analysis, the amounts of hydrogencarbonates in aqueous-phase samples were measured by using a total organic carbon (TOC) analyzer (Rosemount/Dohrmann, Model DC-190). pH values of samples were determined by employing a digital pH meter (Orion, Model 710A) equipped with a Ross combination electrode and ATC probe.

RESULTS AND DISCUSSION

Preliminary experiments of the catalytic liquid-phase hydrogenation of aqueous nitrate solutions are illustrated in Fig. 1. Nitrate reduction was studied by using distilled or tap water as the reaction medium, while nitrogen and carbon dioxide were employed as hydrogen-diluting agents. It can be seen from Fig. 1a that in distilled water nitrate disappears much faster when compared to the temporal courses obtained by using tap water. Lower nitrate disappearance rates observed in the latter case are probably caused by the presence of various salts dissolved in water. Since TOC concentration of drinking water is generally low (below 1 mg/L), it is believed that dissolved organic substances (e.g., humic compounds) would not exhibit any appreciable influence on the reaction kinetics. It is further evident from Fig. 1a that the temporal course of catalytic nitrate reduction is also dependent on the composition of gas mixture continuously bubbled through the reaction suspension. When carbon dioxide is applied as a hydrogen diluting agent, higher nitrate disappearance rates are obtained. Since the nitrate disappearance rate is slightly, but positively, dependent on pH value of the aqueous solution (14), it is concluded that the contributing role of CO_2 to the enhanced reaction rate is associated with the neutralization of stoichiometrically formed hydroxide ions, accordingly to the reactions

$$2OH^- + CO_2 \rightarrow CO_3^{2-} + H_2O \qquad [2]$$

$$CO_3^{2-} + CO_2 + H_2O \rightarrow 2HCO_3^-. \qquad [3]$$

This is further confirmed by the results shown in Fig. 1d, in which the pH value of the aqueous solution is plotted as a function of nitrate conversion. It is obvious that in the presence of CO_2 in the liquid phase, the pH value is practically constant in the entire range of nitrate conversions, despite the nature of the reaction medium; one should note that the difference in equilibrium pH values for distilled and tap water is mostly due to the presence of hydrogencarbonates in drinking water. On the other hand, when nitrogen is used in order to adjust the hydrogen partial pressure in the reactor, the pH value of aqueous solution instantaneously increases at low nitrate conversions, while in the latter stage of reaction it changes only slightly. The obtained pH value–conversion profile is typical of reaction systems possessing low or negligible buffering ability. When distilled water is replaced by tap water, the pH value of the liquid phase is kept constant unless buffer capacity (determined by the concentration of hydrogencarbonates) of tap water is overcome. The above

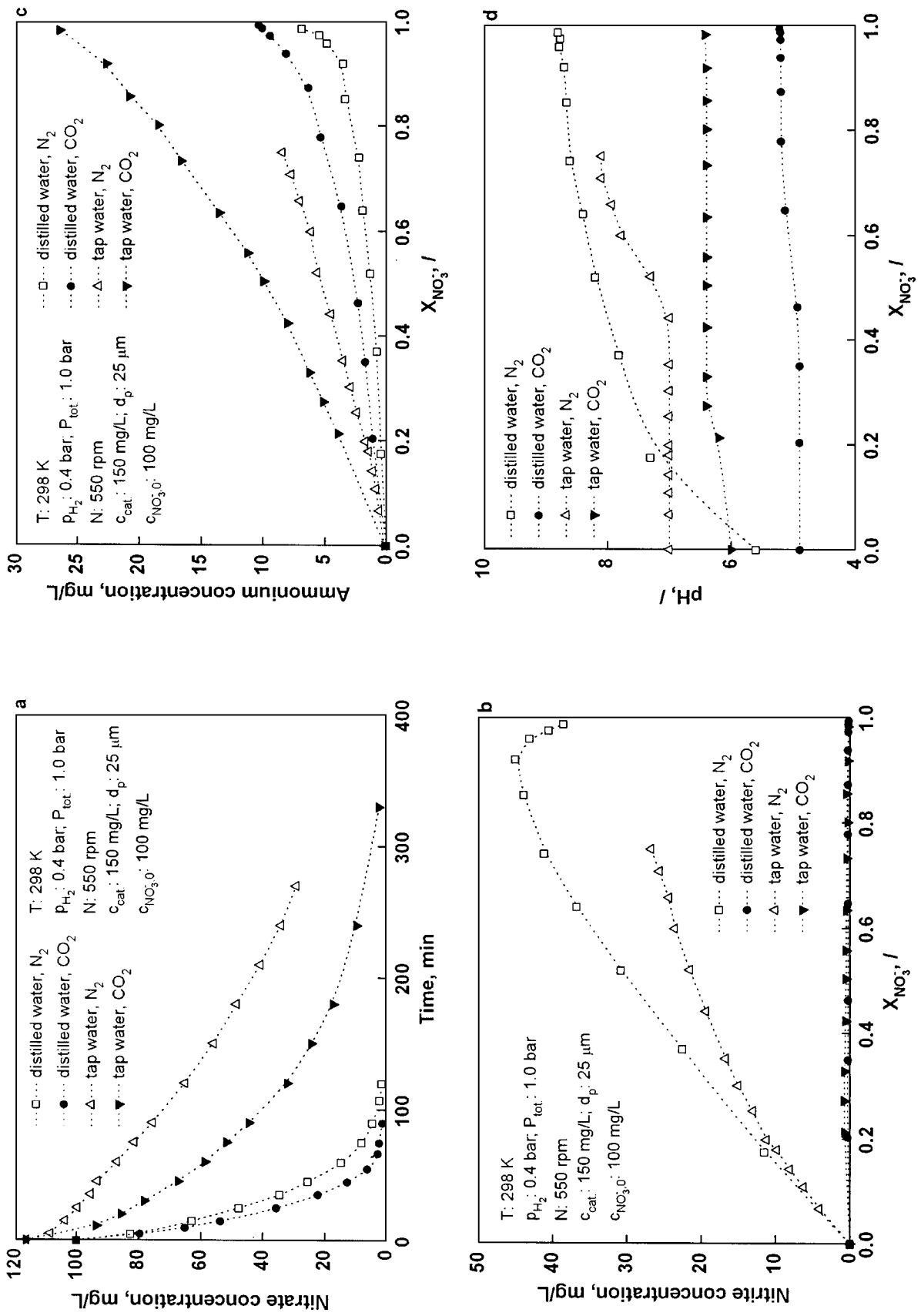

FIG. 1. Nitrate concentration as a function of time (a), nitrite (b) and ammonium (c) ions concentration, and pH value (d) vs nitrate conversion dependencies obtained in the slurry reactor for various reaction media and compositions of the gas phase. Nitrate ion source, KNO_3.

results clearly demonstrate that catalytic nitrate reduction is a pH-dependent reaction, which is in agreement with the observation of other investigators (14). Nevertheless, these data confirm that the investigated reaction is much less sensitive to variations of pH value of the aqueous solution than, e.g., catalytic liquid-phase nitrite reduction (5, 7). Figure 1b illustrates nitrite concentration as a function of nitrate conversion obtained in the slurry reactor for H_2/N_2 and H_2/CO_2 gas mixtures in the presence of distilled or tap water. It is seen that by using nitrogen as the hydrogen-diluting agent, appreciable quantities of nitrites as intermediates are accumulated in the liquid phase during the reaction course. On the other hand, in the presence of CO_2 only small amounts of nitrite were detected in aqueous-phase samples. A comparison of these dependencies with data represented in Fig. 1d has confirmed that the accumulation of nitrite ions in bulk liquid phase could successfully be avoided by carrying out liquid-phase nitrate reduction in slightly acidic solutions, which is also suggested by other authors (2, 13). Appropriate concentrations as a function of nitrate conversion for ammonium ions produced during the course of the catalytic nitrate reduction are shown in Fig. 1c. Minimum formation of ammonium ions is observed for the runs performed in distilled water. When the reactor content was sparged with the H_2/CO_2 gas mixture, higher amounts of ammonium ions were formed. However, one should consider that in this case nitrite accumulation was negligible, which means that the nitrate was directly transformed to nitrogen and ammonia. Furthermore, the mass balance calculations using data plotted in Figs. 1b and 1c confirm that at the given reaction conditions higher values of reaction selectivity are obtained for the runs in which nitrate reduction is carried out by means of the H_2/CO_2 mixture. Finally, the results shown in Fig. 1c also demonstrate that the presence of various ionic species in the liquid-phase enhances the formation of the side product—ammonia. In light of the above discussion, it is concluded that both kinetics and selectivity of the catalytic liquid-phase nitrate hydrogenation are strongly influenced by the presence of salts dissolved in tap water. In further work, a systematic study was performed in order to quantitatively evaluate effects of the most common cations as well as anions in drinking water on the nitrate disappearance rate and ammonia formation.

First of all, catalytic liquid-phase nitrate reduction was studied in the presence of mono-, bi-, and trivalent cations in the aqueous solutions. The results of these experiments are depicted in Fig. 2. It can be seen from Fig. 2a that the nitrate disappearance rate increases in the following order: $K^+ < Na^+ < Ca^{2+} < Mg^{2+} < Al^{3+}$. In our previous investigation (15), a Langmuir–Hinshelwood kinetic formulation in the form of Eq. [4] was successfully employed to fit experimental data which were obtained for a wide range of reactant concentrations and operating conditions in an isothermal slurry reactor by using distilled water as the reaction medium and KNO_3 as the source of nitrate ions:

$$\left(-r_{NO_3^-}\right) = -\frac{dc_{NO_3^-}}{dt \cdot c_{cat.}} = \frac{k_{sr,app.} \cdot K_{NO_3^-} \cdot c_{NO_3^-} \cdot c_{H_2}^{1/2}}{1 + K_{NO_3^-} \cdot c_{NO_3^-}}. \quad [4]$$

It can be thus reasonably supposed that Eq. [4] may satisfactorily describe the process of catalytic nitrate reduction conducted in the presence of other cations. To check for this assumption, the experimental results from Fig. 2a were plotted accordingly to the integrated form of Eq. [4] to see whether straight lines passing through data sets can be obtained. This is illustrated in Fig. 3, where the above condition is undeniably achieved. The experimentally determined values of $K_{NO_3^-}$ and $k_{sr,app.}$ constants, derived by means of a linear regression for different nitrate salts, are listed in Table 3. With these values, Eq. [4] is presented in Fig. 2a by solid curves. These are seen to describe the experimental data very well, thus indicating that the assumptions and the model are reasonable. On the other hand, the high accuracy of the performed measurements is also reflected. It can be seen from Fig. 3 as well as from Table 3 that within an experimental error the physical properties of cations employed in this study exhibit no

TABLE 3

Intrinsic Rate Constants of the Catalytic Liquid-Phase Nitrate Reduction Obtained in the Slurry Reactor for Various Nitrate Salts as Reactant Sources

Salt	Crystal ionic radius, Å[a]	Solvated ionic radius, Å	$10^4 \times \lambda^\circ$, $m^2 \cdot S/mol$[b]	$10^9 \times D$, m^2/s[c]	Actual ionic strength, mmol/L	$10^3 \times K_{NO_3^-}$, L/mg	$k_{sr,app.}$, $mg/(g_{cat.} \cdot min \cdot bar^{1/2})$
KNO_3	1.33	1.75	73.5	1.96	1.6	4.48	87.7
$NaNO_3$	1.24	2.17	50.1	1.33	1.6	4.64	124.2
$Ca(NO_3)_2$	1.00	3.08	59.5	0.79	2.4	4.88	133.5
$Mg(NO_3)_2$	0.72	3.45	53.0	0.71	2.4	4.85	144.5
$Al(NO_3)_3$	0.54	4.22	61.0	0.54	3.2	4.28	310.8

[a] Cation coordination number, 6.
[b] Molar conductivity at infinite dilution of the cation. The values refer to aqueous solutions at $T = 298$ K.
[c] Cation diffusion at infinite dilution. $D = (R \cdot T)/F^2 \cdot (\lambda^\circ/|z|)$.

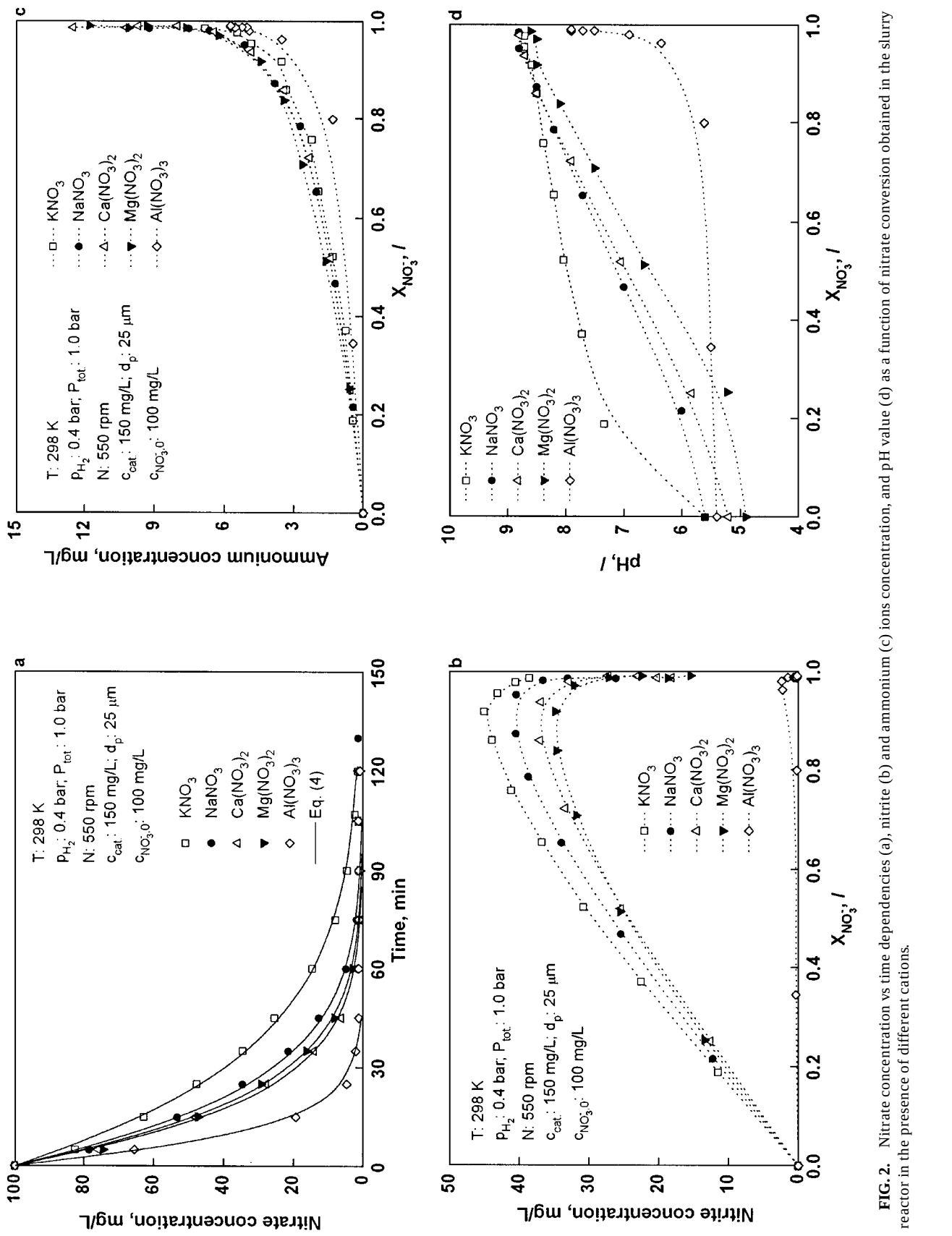

FIG. 2. Nitrate concentration vs time dependencies (a), nitrite (b) and ammonium (c) ions concentration, and pH value (d) as a function of nitrate conversion obtained in the slurry reactor in the presence of different cations.

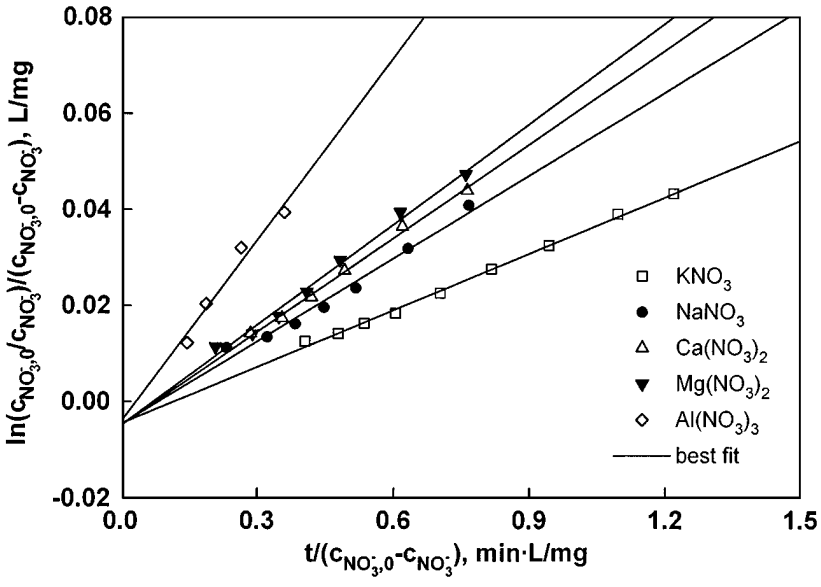

FIG. 3. Test of the proposed Langmuir–Hinshelwood kinetic model.

influence on the nitrate adsorption constant; it is thus concluded that the latter is only a function of catalyst properties and actual reaction conditions. Furthermore, an attempt was made to correlate the values of apparent surface reaction rate constant, $k_{sr,app.}$, with various physical properties of cations in the reaction medium, such as electronegativity (or electron affinity) of elements, crystal ionic radius, radii of solvated ions, and ionization potential. It has been discovered that among the listed properties the apparent surface reaction rate constant changes proportionally with the ionization potential of a cation present in the aqueous solution, which is clearly demonstrated in Fig. 4. The deviation from the regression curve, which is observed for Mg^{2+}, is attributed to the low solubility product constant of $Mg(OH)_2$ ($K_{sp} = 5.61 \times 10^{-12}$ at $T = 298$ K (18)). Due to the production of hydroxide ions during the reaction course, this value is easily exceeded; consequently, $Mg(OH)_2$ precipitates, which reduces the concentration of Mg^{2+} ions in the liquid phase, and correspondingly decreases the polarization of the hydroxide ions produced. It has been found that at $X_{NO_3^-} = 0.5$ the concentration of dissolved magnesium ions decreases by about 20%, which is very close to the deviation of measured $k_{sr,app.}$ for $Mg(NO_3)_2$ from the best fit curve in Fig. 4. For instance, the value of K_{sp} of

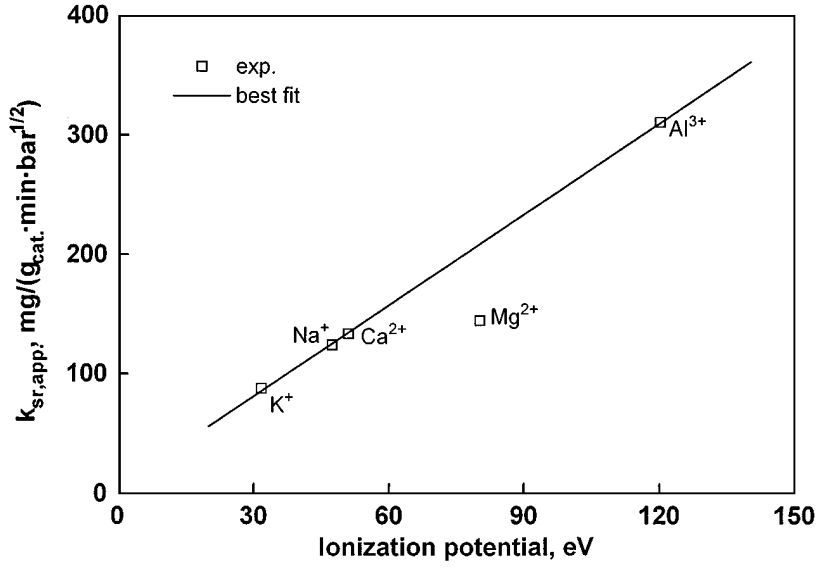

FIG. 4. Apparent surface reaction rate constant, $k_{sr,app.}$, as a function of ionization potential over the Pd–Cu bimetallic catalyst.

calcium hydroxide is higher by about six orders of magnitude; thus, no precipitation of $Ca(OH)_2$ occurred in any of these hydrogenation experiments.

Figure 2b shows nitrite concentration as a function of nitrate conversion obtained in the slurry reactor for various nitrate salts. It is evident that the maximum concentration of accumulated nitrite ions decreases in the following order: $K^+ > Na^+ > Ca^{2+} > Mg^{2+} > Al^{3+}$. It is very interesting that in the presence of aluminium cations in the aqueous solution, nitrite accumulation is almost negligible, which further leads to lower formation of ammonium ions (Fig. 2c). However, in the presence of mono- and bivalent cations in the aqueous phase, up to twice higher amounts of ammonia were formed; at the used reaction conditions, almost no difference in the respective profiles shown in Fig. 2c can be observed, which was also confirmed by calculating reaction selectivities at different nitrate conversions. Furthermore, Fig. 2d demonstrates the pH values of the aqueous solution as a function of nitrate conversion for various nitrate salts. It is seen that in the presence of K^+ ions, the pH value changes abruptly in the very first stage of the reaction, while for cations with higher ionization potentials there exist inflection points in the respective profiles which are located at higher nitrate conversions. Furthermore, when catalytic nitrate reduction was conducted in the presence of Al^{3+} cations, the pH value of the aqueous solution was kept constant up to $X_{NO_3^-} = 0.8$, which might be ascribed to the formation of $[Al(OH)_4]^-$ complex. The above described experimental observations and comparison of data illustrated in Fig. 2 allude that during the liquid-phase nitrate reduction carried out in the presence of various nitrate salts, the catalyst surface becomes negative to a different extent; however, the influence of repulsion forces between the catalyst surface and ions in the aqueous solution on the reaction course is more distinctive for nitrites than for nitrates (5, 7, 14). It is furthermore believed that both the nitrate disappearance rate and the accumulation of nitrite ions in the bulk liquid phase are in close connection with the concentration of hydroxide ions in the Helmholtz (i.e., inner or compact) layer surrounding catalyst particles. As Figs. 2a and 2b suggest, higher affinity of cations toward hydroxide ions enhances the transformation of nitrate and nitrite ions. The desorption rate of hydroxide ions from the Pd–Cu active sites obviously increases with higher polarization ability of cations present in the liquid phase. While the nitrate adsorption constant is independent of the cation ionization potential, its effect on the apparent surface reaction rate constant is substantial (Fig. 3). With this respect, one can also conclude that faster removal of hydroxide ions from the Helmholtz layer into the diffuse layer and the bulk liquid phase consequently leads to faster regeneration of the catalyst surface. In other words, a larger number of Pd–Cu sites can be accessed by nitrates and nitrites in the subsequent reaction cycles. Since the inflection points of pH profiles (Fig. 2d) are shifted toward higher nitrate conversions by increasing the ionization potential of a cation, it can be further speculated that hydroxide ions are not freely mobile in the liquid phase; due to the attraction forces, they are found in the vicinity of cations.

The dependencies shown in Fig. 2a and the validity of the proposed L–H kinetic model (Eq. [4]) demonstrate that the measured nitrate conversions are not influenced by the interstitial and intraparticle mass-transfer resistances. This is further confirmed by a comparison of diffusivities of the cations at infinite dilution (18) with appropriate values of $k_{sr,app.}$ in Table 3, which shows that the nitrate disappearance rate is not affected by the mobility of ionic species within the catalyst pores. When homogeneous reactions, either catalyzed or uncatalyzed, are carried out in aqueous solutions, one can generally observe that for cations of the same valence there is a marked parallelism between the decrease in the reaction rate constant and the decrease in the limiting conductance of the cations at infinite dilution (19). However, in this work an opposite trend has been observed, which indicates that the liquid-phase nitrate hydrogenation is determined only by the processes taking place at the catalyst surface or in the Helmholtz layer. It can be seen from the data provided in Table 3 that the aluminium ion has greater solvation than the potassium ion in aqueous solutions at the same concentration and temperature (20). This means that in aqueous solutions the aluminium ion would be more bulky than the potassium ion, although the unsolvated aluminium ion has a radius of 0.54 Å and the unsolvated potassium ion has a radius of 1.33 Å. Therefore, one could reasonably assume that the hydrated aluminium ion would cause less polarization of the hydroxide ion than the potassium ion would, which results in lower nitrate disappearance rate. As discussed above, an opposite effect of the cation present in the liquid phase on the reaction rate was observed. Since the apparent surface reaction rate constant, $k_{sr,app.}$, increases by the decrease of the ionic crystal radius, it might be tentatively concluded that the ionic species found in the Helmholtz layer are less solvated than in the bulk liquid phase, which is also suggested by other authors (21). Accordingly to the observed influence of cations on the reaction kinetics, it is believed that in this layer the cations are surrounded only by one solvation sheet. Furthermore, homogeneous ionic reactions are markedly influenced by the presence of a salt in the aqueous solution. The effect of ionic strength on the reaction rate constant is quantitatively described by the Brønsted–Debye–Hückel equation, which says that the rate of a reaction between two anions or two cations will increase with a square root of ionic strength, whereas for a reaction of oppositely charged ions it will decrease (19, 22). In the case of ion–dipolar molecule reactions, the logarithmic value of the reaction rate constant is generally a linear function of the ionic strength (19). It can be seen from the results shown

in Table 3, as well as from the forthcoming discussion, that in the present investigation ionic strength exhibits no direct influence on the intrinsic rate constants. Consequently, the Debye length (being in the range of 15–80 Å), and hence the spatial extension of the double layer, also have no effect on the catalytic liquid-phase nitrate hydrogenation. The drinking water which was used in this study mostly involved Ca^{2+} and Mg^{2+} ions. On the basis of the above discussion, one could expect that the catalytic nitrate reduction would occur faster in this reaction medium. Figure 1 indicates that the contributing role of bivalent cations in the reaction rate is probably surpassed by the presence of various anions in the liquid phase.

The investigation was continued by studying the effects of those anions on the catalytic nitrate reduction that might be present in drinking waters at the highest concentrations (i.e., chlorides, hydrogencarbonates and sulfates). First, the influence of various chlorides on reaction kinetics and selectivity was examined. In all these runs, KNO_3 was used as a source of nitrate ions. The concentration of chloride ions was equal to 200 mg/L, which is the maximum admissible concentration for drinking water. The obtained results are plotted in Fig. 5. It is obvious that in the presence of chlorides the nitrate disappearance rate increases, while the nature of cations found in the aqueous solution has no significant effect on the temporal course of nitrate reduction. It was further observed that bivalent cations slightly reduce the maximum concentration of nitrites accumulated in the liquid phase. On the other hand, the ammonium concentration vs nitrate conversion profiles were found to be identical in all these runs, thus suggesting that despite the large crystal ionic radius of 1.8 Å (18) the chloride ion does not contribute to the enhanced formation of ammonium ions, which was otherwise observed for nitrate reductions carried out in drinking water (Fig. 1). The pH value of the aqueous phase as a function of nitrate conversion is illustrated in Fig. 5b. It is evident that in the presence of chloride ions, the increase in pH value is slower when compared to the run in which only KNO_3 was dissolved in the aqueous solution. For all chloride salts, the pH value changes similarly during the reaction course, which further leads to identical nitrate concentration–time profiles shown in Fig. 5a. The kinetic analysis of the respective data shows that in the presence of chlorides in the reaction suspension, the adsorption constant for the nitrate ion, $K_{NO_3^-}$, is higher and equal to 0.00769 L/mg, while the apparent surface reaction rate constant, $k_{sr,app.}$, was found to be 93 mg/($g_{cat.} \cdot min \cdot bar^{1/2}$)). Figure 5a demonstrates good agreement between the measured and calculated values and thus confirms the validity of the proposed L–H kinetic model (Eq. [4]) even in the presence of chlorides in the reaction medium. Based on the results shown in Fig. 5b, one can speculate that the chloride ion, due to its electronegativity, positively modifies the concentration and strength of Brønsted acidic sites, which promotes the neutralization of produced hydroxide ions to a particular extent. Finally, the chloride ion, otherwise known as a catalyst poison, does not act as an inhibitor of the destructive hydrogenation of nitrate ions.

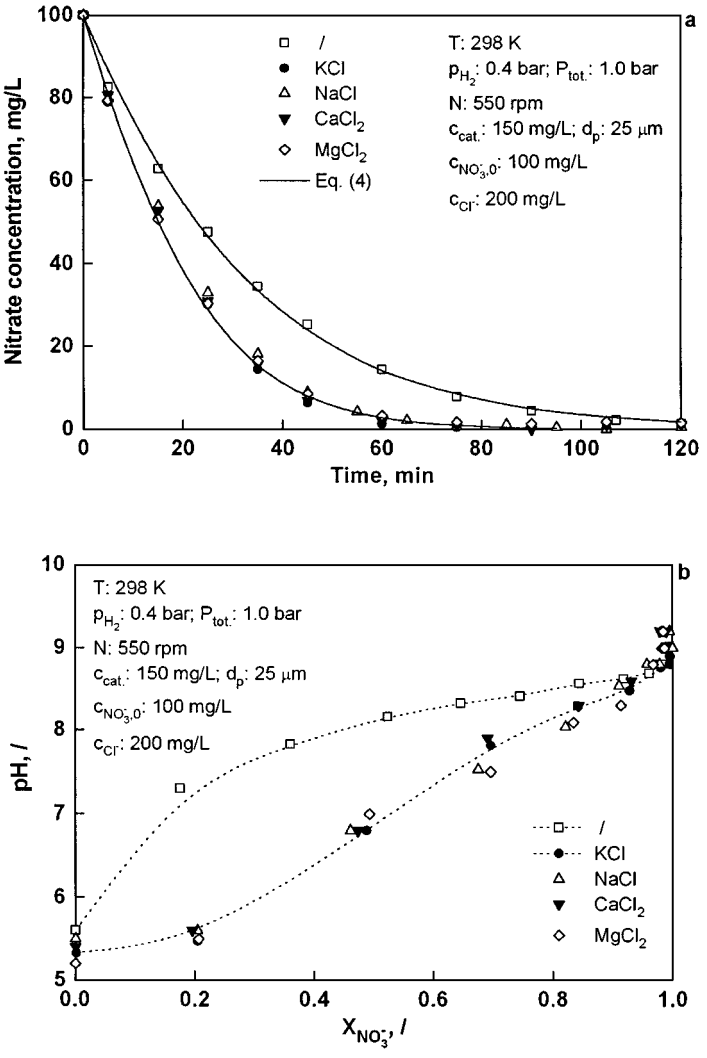

FIG. 5. Nitrate concentration as a function of time (a) and pH value vs NO_3^- conversion dependencies (b) in the course of catalytic liquid-phase nitrate reduction in the presence of chlorides. Nitrate ion source, KNO_3.

Similar results as described above for chlorides were obtained also in the presence of various sulfate salts in the liquid phase. In these experiments, the concentration of added sulfate ions was equal to the maximum admissible concentration for drinking water (i.e., 200 mg/L). It is obvious from Fig. 6a that at the employed reaction conditions the sulfate ion exhibits no retarding effect on the kinetics of the reaction under consideration. Furthermore, the sulfate anion (with the crystal ionic radius of 2.3 Å (18)) does not influence in any way the formation of the by-product ammonia. Figure 6b shows the pH value of the aqueous solution as a function of nitrate conversion in the presence of various

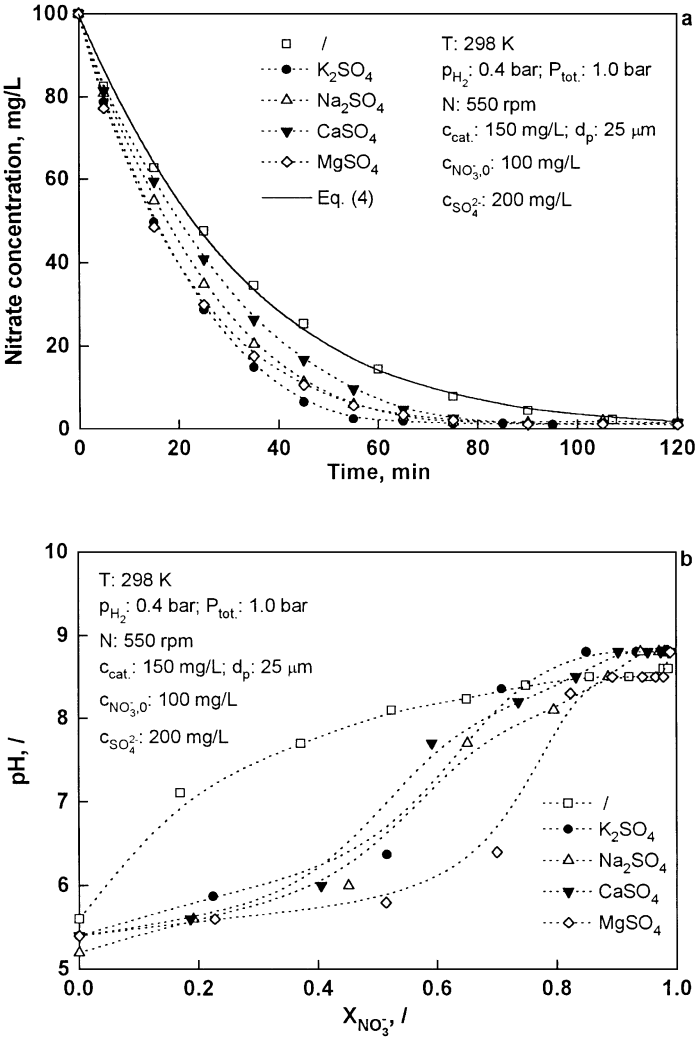

FIG. 6. Nitrate concentration vs time dependencies (a) and pH value as a function of nitrate conversion (b) obtained in the slurry reactor in the presence of various sulfates. Nitrate ion source, KNO_3.

sulfates. In these cases, the pH value changes moderately in the first part of the reaction, while at higher nitrate conversions sudden variations in pH-conversion profiles can be seen. It is common to all profiles that in the final reaction stage the pH asymptotically approaches values close to 9. It can be observed in Fig. 6b that for different sulfates the inflection points in the profiles are located at various nitrate conversions, which might be attributed to different buffer capacities of the reaction suspensions. As with chlorides, also in this case the nature of cations in the aqueous solution has practically no measurable influence on the catalytic nitrate reduction. It should be noted that the concentration of sulfate (and chloride) ions was constant during the catalytic nitrate reduction, which was confirmed by additional UV/VIS–FIA analyses. Correspondingly, under the given operating conditions, formation of sulfite ions can be excluded. Based on the above discussion, it is stated that permanent hardness of drinking water has no inhibitive effect on either the extent of nitrate reduction or reaction selectivity.

Since permanent hardness of tap water exhibits no retarding influence on the nitrate disappearance rate, further experiments were carried out in which the effect of temporary hardness on the reaction course was investigated. For that purpose, different quantities of $KHCO_3$ were added to the reaction suspension prior to starting the reduction runs. The concentrations of hydrogencarbonate ions were in the range 0–500 mg/L. The auxiliary TOC analysis revealed that the inorganic carbon content was constant during the reaction course. It is demonstrated in Fig. 7a that the nitrate disappearance rate is appreciably decreased in the presence of HCO_3^- ions. The inhibitive effect of these species on the reaction kinetics might be attributed to the identical structures of NO_3^- and HCO_3^- ions. They are both planar, and the angles between the N–O and C–O bonds are equal to 120°. It can be thus reasonably believed that HCO_3^- anions competitively adsorb to the same active sites on the surface of the Pd–Cu bimetallic catalyst. Similarly, one can also explain the inertness of the sulfate ion. It was mentioned before that this anion has no negative effect on the nitrate disappearance rate, which is probably due to the tetrahedral structure of the sulfate ion. It can be thus concluded that the catalytic nitrate hydrogenation, when conducted in drinking water, is influenced only by those ionic species the structure of which is equal to the one of the nitrate ion. It has been demonstrated earlier that the size of ions present in the liquid phase is not essential. Figure 7b shows the concentration of intermediate nitrite ions as a function of nitrate conversion in the absence as well as in the presence of hydrogencarbonates, while Fig. 7c illustrates the corresponding concentrations of produced ammonium ions vs nitrate conversion dependencies. It is evident in Fig. 7b that in the presence of HCO_3^- ions the peak nitrite concentrations are lower than the one measured in the absence of HCO_3^-. On the contrary, it arises from Fig. 7c that in the presence of hydrogencarbonates much higher quantities of ammonium ions are formed. It should be pointed out that for any concentration of HCO_3^- ions in the aqueous solution, pH value vs nitrate conversion profiles were identical to the one for $c(HCO_3^-) = 0$ (Fig. 2d). According to these observations, one can propose that HCO_3^- hinders the diffusion of nitrite ions into the bulk liquid phase. It is further believed that the same species also hinder the counterdiffusion of nitrogen from the catalyst pores, thus leading to enhanced production of ammonia. It is interesting to point out that in the presence of hydrogencarbonates in the aqueous solution the proposed L–H kinetic model (Eq. [4]) is not valid any longer. Figure 7a suggests that the reaction undergoes a simple first-order kinetics of power-law type. Consequently, an influence of HCO_3^- anions on the intrinsic rate constants (Eq. [4]) cannot be quantitatively evaluated.

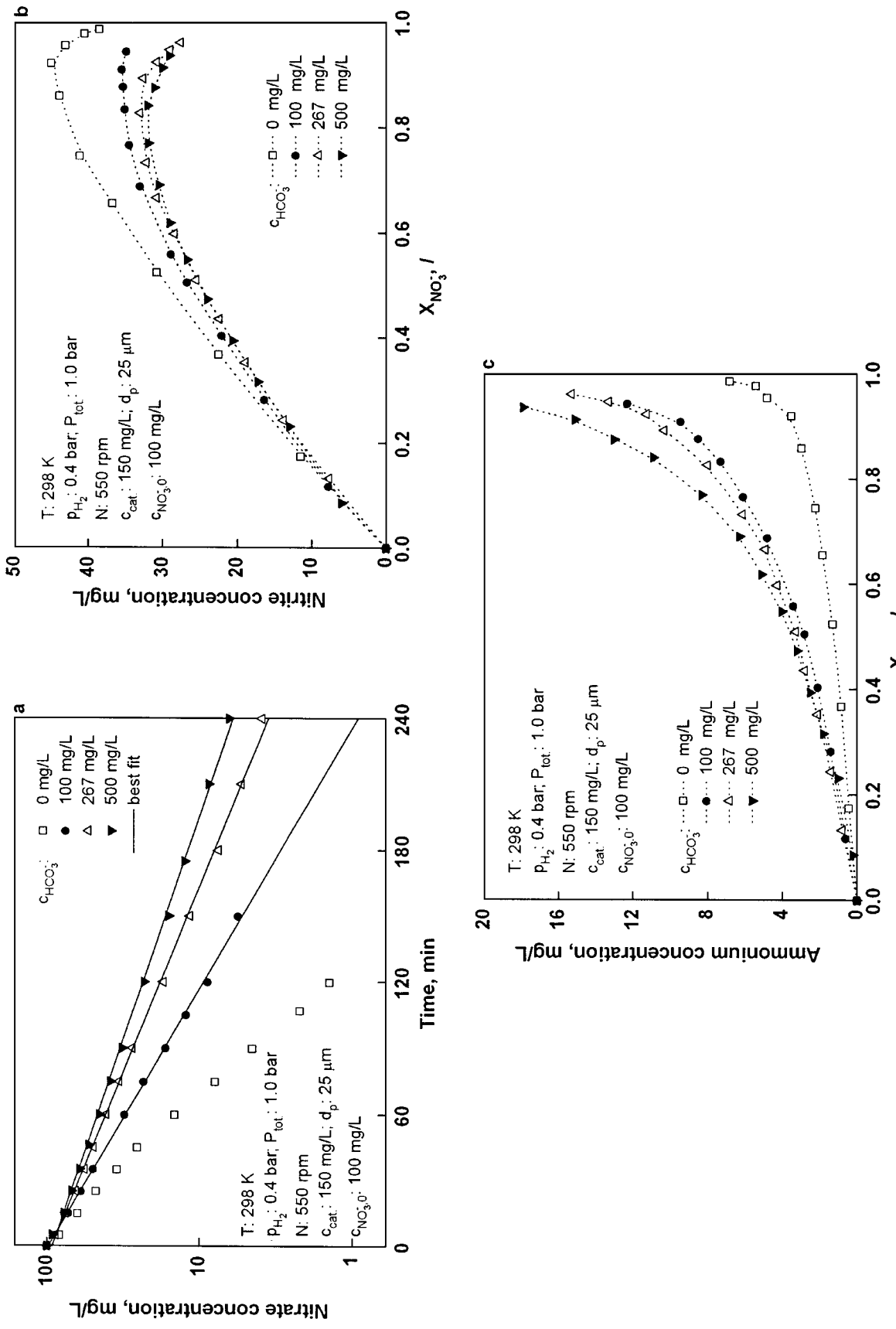

FIG. 7. Nitrate concentration–time profiles (a) and nitrite (b) and ammonium (c) ions concentrations as a function of nitrate conversion obtained in the course of catalytic nitrate hydrogenation using different quantities of $KHCO_3$. Nitrate ion source, KNO_3.

Nevertheless, it is believed that the drastic change in the reaction kinetics of the catalytic nitrate reduction is due to additional resistances in the adsorption processes of nitrates on the catalyst surface.

Additional runs were performed in which $KHCO_3$ was replaced with other hydrogencarbonates. When $NaHCO_3$ was used as a source of hydrogencarbonate ions, the nitrate removal was even more retarded. This finding suggests that a cation with smaller crystal ionic radius enhances the adsorption of HCO_3^- to the Pd–Cu active sites and consequently reduces the reactant's concentration on the catalyst surface. Further comparison of the results obtained in these two runs shows that the properties of cations are not significant for the accumulation of nitrite ions; on the other hand, in the presence of $NaHCO_3$ in the slurry, formation of ammonium ions decreases by about 30%, which means that in comparison to the potassium ion, the sodium cation hinders nitrogen desorption from the catalyst surface to a lesser extent. Among the bivalent hydrogencarbonates, only the influence of $Ca(HCO_3)_2$ on the reaction course was investigated. Due to the low solubility product constant of $Mg(OH)_2$, pure $Mg(HCO_3)_2$ cannot be synthesized. $Ca(HCO_3)_2$ was prepared *in situ* by dissolving an appropriate amount of $CaCO_3$ in the aqueous solution saturated with CO_2. In this case, liquid-phase nitrate reduction was carried out by means of hydrogen diluted by CO_2; the latter prevented coprecipitation of $Ca(OH)_2$ that might occur due to the increase in pH value during the reaction course. In the presence of $Ca(HCO_3)_2$, the nitrate destruction was even more retarded than in the presence of monovalent cations, which again confirms that a cation with smaller crystal ionic radius negatively influences the catalytic nitrate reduction. Some liquid-phase nitrate hydrogenation experiments were performed in which an equimolar amount of K_2CO_3 was introduced into the aqueous solution instead of $KHCO_3$. In these runs, the pH value of the liquid phase was maintained constant with reaction time in the range 10.1–10.2. Due to the dynamic equilibrium between HCO_3^- and CO_3^{2-} anions ($pK_a = 10.25$ at $T = 298$ K), the molar concentration ratio was close to 1 (in other words, $c(HCO_3^-) \approx 134$ mg/L). The comparison of the obtained nitrate concentration vs time dependence with the corresponding results shown in Fig. 7a alludes that the nitrate disappearance rate is mostly determined by the concentration of hydrogencarbonates present in the aqueous solution, while carbonate anions exhibit negligible effect on both the temporal course of the reaction as well as on the production of ammonium ions. Based on the above discussion, it can be concluded that in drinking water containing mostly calcium and magnesium hydrogencarbonates in appreciable quantities, nitrate removal by employing the catalytic liquid-phase hydrogenation might be considerably hindered.

Liquid-phase reduction experiments were also conducted in order to find out the effects of gas- and liquid-phase compositions on the catalytic nitrite hydrogenation. The results are illustrated in Fig. 8; in the runs represented, the hydrogen partial pressure was equal to 0.1 and 0.4 bar, respectively. It can be seen in Fig. 8a that the nitrite ion disappears very fast when carbon dioxide is employed as a hydrogen-diluting agent. This is attributed to the low pH value of the aqueous solution, which was kept constant at pH = 4.9–5.0 during the entire reaction course. When hydrogen partial pressure was equal to 0.4 bar, the nitrite ion was completely transformed within a few minutes. On the other hand, when a hydrogen–nitrogen gas mixture was used as a reducing agent, the nitrite disappearance rate was still high in the very first stage of the reaction. Simultaneously, the pH value of the aqueous solution changed abruptly due to the formation of hydroxide ions, which made the surface of Pd–Cu particles negatively charged. Consequently, due to repulsion forces, the nitrite disappearance rate ceased, which is in agreement with the observations of other authors (5, 7). It can be further seen from Fig. 8a that at the used operating conditions, composition of the reaction medium has no impact on the nitrite disappearance rate. This experimental finding was expected, since with respect to the structure of the nitrite ion there is no species available in tap water which could competitively adsorb to the Pd–Cu active sites. Figure 8b clearly shows that the formation of ammonium ions increases by increasing the hydrogen partial pressure. Furthermore, ammonia production is favored under pH noncontrolled conditions or when the nitrite reduction is carried out in tap water. It is believed that in the latter case enhanced ammonia formation can be attributed to the presence of hydrogencarbonate anions, hindering the desorption of nitrogen from the catalyst surface. At the end, investigations were conducted in order to determine the role of the nitrate ion during the course of the catalytic liquid-phase nitrite reduction. In this case, the monometallic Pd (5 wt%)/γ-Al_2O_3 catalyst was used. It is well documented that this solid is a good catalyst that promotes nitrite reduction; however, it is completely inactive for the liquid-phase nitrate transformation to nitrogen (5, 9, 10). In these runs, the initial nitrite concentration was equal to 74 mg/L, and the hydrogen partial pressure was set to 0.4 bar; all other operating parameters were equal to those listed in the caption of Fig. 8. When only $NaNO_2$ was present in the aqueous solution at the beginning of reduction run, under the given experimental conditions 4.1 mg/L of ammonium ions were found in the liquid phase after the transformation of nitrites was completed. However, in the presence of nitrite as well as nitrate ions (100 mg/L) in the aqueous phase the formation of ammonium ions was appreciably enhanced; at the end of reaction, 10.5 mg/L of ammonium ions were detected in the aqueous solution. In light of this experimental finding, it can be concluded that the nitrate ion, analogously to the hydrogencarbonate anion, reduces selectivities of the concerned reactions. Therefore,

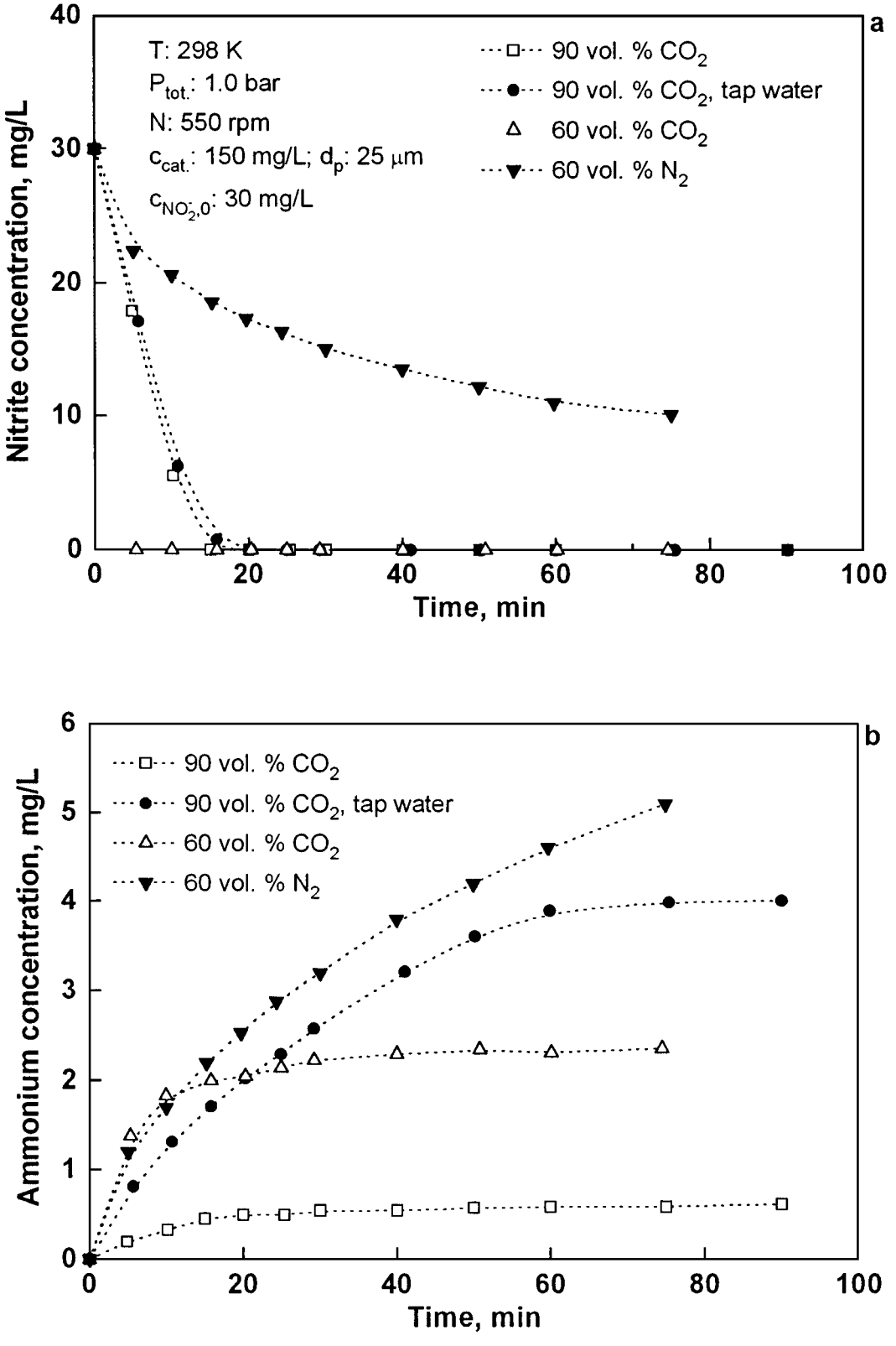

FIG. 8. Nitrite (a) and ammonium (b) ions concentration as a function of time obtained in the slurry reactor using different reaction media and gas mixtures. Nitrite ion source, $NaNO_2$.

TABLE 4

Concentrations of Pd and Cu Ions, Leached from the Pd–Cu Bimetallic Catalyst at Different pH Values

pH, /	c_{Pd}, mg/L	c_{Cu}, mg/L
2.0	42	11.7
5.2	<0.3	<0.1
8.1	<0.3	<0.1
10.0	<0.3	<0.1

it is believed that in the process of catalytic liquid-phase hydrogenation of aqueous nitrate solutions the NO_3^- ion plays a dual role: (i) it acts as the reactant; and (ii) it hinders the desorption of intermediate and final products from the surface of supported Pd monometallic and Pd–Cu bimetallic catalysts.

Finally, the chemical stability of the Pd–Cu bimetallic catalyst was tested. For that purpose, the amounts of leached palladium and copper ions in aqueous-phase samples were determined by means of an ICP–AES method. In all samples, the concentrations of metal ions were found to be below the detection limits of both elements. Furthermore, the chemical analysis of fresh and used catalyst samples confirmed that no dissolution of active components took place during the above-described experiments. Also, cold oxidation of Cu by ammonia, leading to the appearance of Schweitzer's blue liquor, was not observed. To elucidate the chemical resistance of the Pd–Cu catalyst, long-term stability tests were additionally performed. The catalyst samples were exposed to aqueous solutions of various pH values. For all pH values except pH 2, the concentrations of Pd and Cu ions were found to be below the detection limit of the applied analytical technique (Table 4). The high concentrations of Pd and Cu dissolved in the liquid phase at pH 2 are associated with the instability of alumina support in aqueous solutions with a pH value below 3 (23). Nevertheless, these experimental findings reflect high chemical stability of the Pd–Cu bimetallic catalyst under neutral and slightly acidic conditions, which is with this respect undoubtedly convenient for nitrate removal from drinking water streams.

CONCLUSIONS

In the absence of HCO_3^- ions in the aqueous phase, the rate of nitrate disappearance is well described by a rate equation of the Langmuir–Hinshelwood type, which accounts for both noncompetitive and equilibrium nitrate and dissociative hydrogen adsorption steps. The results of reduction runs performed by using model aqueous solutions demonstrate that the nitrate disappearance rate is proportional to the ionization potential of cations present in the liquid phase, while physical properties of cations have no measurable impact on the nitrate adsorption constant. Cations with higher polarization ability enable faster regeneration of the catalyst surface and consequently increase the concentration of active sites accessible to NO_3^- and NO_2^- ions. Chlorides and sulfates in the reaction medium moderately increase the reaction rate, which is ascribed to the modification of acidic centers on the catalyst surface. The nitrate disappearance rate is decreased in the presence of hydrogencarbonates, which is attributed to the competitive adsorption of NO_3^- and HCO_3^- ions to the Pd–Cu active sites. Adsorption of the latter species is favored in the presence of cations of smaller crystal radii. Due to the slower desorption of intermediates and nitrogen from the catalyst surface, temporary hardness of tap water accelerates the formation of ammonia as a side product. It is confirmed that for the purification of drinking water much higher reaction selectivity can be achieved when total hardness of the reaction medium is almost equal to the permanent hardness and when a H_2/CO_2 gas mixture is employed as a reducing agent. The catalyst comprising Pd and Cu metallic phases exhibits high chemical stability under the experimental conditions employed. However, the composition of bimetallic solids should be optimized in order to decrease or avoid the formation of NH_4^+ ions.

APPENDIX: NOTATION

$c_{NO_3^-}$	nitrate concentration, mg/L
$c_{cat.}$	catalyst concentration in slurry reactor, mg/L
d_p	average catalyst particle diameter, μm
D	diffusion coefficient in liquid-phase, m^2/s
$k_{sr,app.}$	apparent surface reaction rate constant, $mg/(g_{cat.} \cdot min \cdot bar^{1/2})$
$K_{NO_3^-}$	equilibrium nitrate adsorption constant, L/mg
N	stirrer speed, rpm
p_{H_2}	hydrogen partial pressure, bar
$P_{tot.}$	total operating pressure, bar
$(-r_{NO_3^-})$	nitrate disappearance rate, $mg/(g_{cat.} \cdot min)$
t	reaction time, min
T	reaction temperature, K
$X_{NO_3^-}$	nitrate conversion, /
z	charge of ion, /
0	initial
λ°	molar conductivity at infinite dilution, $m^2 \cdot S/mol$

ACKNOWLEDGMENT

The authors thank the Nikki-Universal Co., Ltd. (Tokyo, Japan), for providing the alumina support used in the present study.

REFERENCES

1. Canter, L. W., "Nitrates in Groundwater." CRC Press, Boca Raton, FL, 1996.

2. Sell, M., Bischoff, M., and Bonse, D., *Vom Wasser* **79**, 129 (1992).
3. Kapoor, A., and Viraraghavan, T., *J. Environ. Eng.* **123**(4), 371 (1997).
4. Vorlop, K. D., Tacke, T., Sell, M., and Strauss, G., DE 3830850 A1, European Patent Office, September 10, 1988.
5. Vorlop, K. D., and Tacke, T., *Chem. Ing. Tech.* **61**(10), 836 (1989).
6. Hörold, S., Vorlop, K. D., Tacke, T., and Sell, M., *Catal. Today* **17**, 21 (1993).
7. Hörold, S., Tacke, T., and Vorlop, K. D., *Environ. Tech.* **14**, 931 (1993).
8. Wärnå, J., Turunen, I., Salmi, T., and Maunula, T., *Chem. Eng. Sci.* **49**(24B), 5763 (1994).
9. Pintar, A., and Kajiuchi, T., *Acta Chim. Slovenica* **42**(4), 431 (1995).
10. Batista, J., Pintar, A., and Čeh, M., *Catal. Lett.* **43**, 79 (1997).
11. Strukul, G., Pinna, F., Marella, M., Meregalli, L., and Tomaselli, M., *Catal. Today* **27**, 209 (1996).
12. Prüsse, U., Hörold, S., and Vorlop, K. D., *Chem. Ing. Tech.* **69**(1–2), 93 (1997).
13. Prüsse, U., Kröger, S., and Vorlop, K. D., *Chem. Ing. Tech.* **69**(1–2), 87 (1997).
14. Tacke, T., and Vorlop, K. D., *Chem. Ing. Tech.* **65**(12), 1500 (1993).
15. Pintar, A., Batista, J., Levec, J., and Kajiuchi, T., *Appl. Catal. B: Environ.* **11**, 81 (1996).
16. Strohmeier, B. R., Leyden, D. E., Field, R. S., and Hercules, D. M., *J. Catal.* **94**, 514 (1985).
17. Cawse, P. A., *Analyst* **92**, 311 (1967).
18. Lide, D. R. (Ed.), "CRC Handbook of Chemistry and Physics," 73rd ed. CRC Press, Boca Raton, FL, 1992.
19. Amis, E. S., "Solvent Effects on Reaction Rates and Mechanisms." Academic Press, New York, 1966.
20. Monk, C. B., "Electrolytic Dissociation." Academic Press, London, 1961.
21. Marcus, Y., "Ion Solvation." Wiley, Chichester, 1985.
22. Espenson, J. H., "Chemical Kinetics and Reaction Mechanisms," 2nd ed., p. 197. McGraw–Hill, New York, 1995.
23. Ponec, V., and Bond, G. C., "Catalysis by Metals and Alloys." Elsevier, Amsterdam, 1995.